

Curcumin protects murine lung mesenchymal stem cells from H₂O₂ by modulating the Akt/Nrf2/HO-1 pathway

Journal of International Medical Research
48(4) 1–11

© The Author(s) 2020

Article reuse guidelines:

sagepub.com/journals-permissions

DOI: 10.1177/0300060520910665

journals.sagepub.com/home/imr



Shiwen Ke¹, Yuanbing Zhang², Zhihui Lan²,
Shaofeng Li², Wei Zhu³ and Liangji Liu² 

Abstract

Objectives: Oxidative stress within the idiopathic pulmonary fibrosis microenvironment decreases the survival of lung mesenchymal stem cells (LMSCs), resulting in disease progression. Herein, the effects of curcumin (CUR) against hydrogen peroxide (H₂O₂)-mediated damage to murine LMSCs were examined.

Methods: Apoptosis, reactive oxygen species, and mitochondrial membrane potential were detected by flow cytometry. Protein levels of B-cell lymphoma-2 (Bcl-2), Bcl-2 associated x (Bax), cleaved caspase-3, protein kinase B (PKB/Akt), phosphorylated-Akt, nuclear factor erythroid-2-related factor 2 (Nrf2), and heme oxygenase-1 (HO-1) were evaluated by western blot analysis.

Results: Apoptosis rates in the 2.5, 5, and 10 μM CUR groups were 23.27% ± 0.31%, 14.87% ± 0.41%, and 6.47% ± 0.50%, respectively, all of which were lower than in the H₂O₂ group (24.46% ± 1.35%). Reactive oxygen species levels were decreased, while mitochondrial membrane potential levels were increased in concentration-dependent manners in the CUR groups compared with the H₂O₂ group. Compared with the H₂O₂ group, all CUR groups showed reduced cleaved caspase-3 expression, increased Nrf2 and HO-1 expression, and increased Bcl-2/Bax and p-Akt/Akt ratios.

Conclusions: The protective effects of CUR against H₂O₂-mediated damage in murine LMSCs may be mediated through the Akt/Nrf2/HO-1 signaling pathway.

³The Second Clinical Medical School, Guangzhou University of Chinese Medicine, Guangzhou, Guangdong, China

Corresponding author:

Liangji Liu, Department of Respiration, Affiliated Hospital of Jiangxi University of Traditional Chinese Medicine, No. 445 Bayi Avenue, Nanchang, Jiangxi, 330006, China.
Email: llj6505@163.com

¹School of Clinical Medicine, Jiangxi University of Traditional Chinese Medicine, Nanchang, Jiangxi, China

²Department of Respiration, Affiliated Hospital of Jiangxi University of Traditional Chinese Medicine, Nanchang, Jiangxi, China



Creative Commons Non Commercial CC BY-NC: This article is distributed under the terms of the Creative

Commons Attribution-NonCommercial 4.0 License (<https://creativecommons.org/licenses/by-nc/4.0/>) which permits non-commercial use, reproduction and distribution of the work without further permission provided the original work is attributed as specified on the SAGE and Open Access pages (<https://us.sagepub.com/en-us/nam/open-access-at-sage>).

Keywords

Curcumin, lung mesenchymal stem cells, Akt/Nrf2/HO-1 signaling pathway, oxidative stress, apoptosis, idiopathic pulmonary fibrosis

Date received: 31 July 2019; accepted: 23 January 2020

Introduction

Idiopathic pulmonary fibrosis (IPF) is a chronic and progressive lung disease with a mean survival time of 2–5 years.¹ Although two agents, pirfenidone and nintedanib, have been shown to decrease the physiological progression of IPF and are likely to improve progression-free survival, patient outcomes remain unsatisfactory.² Recently, cell replacement therapies have attracted significant attention as a better alternative method of treating IPF.^{3–5} Mesenchymal stem cells (MSCs) are a type of adult stem cell that can repair tissues, regulate immunity, and inhibit fibrosis.⁶ As such, lung MSCs (LMSCs) are considered the most effective treatment for IPF; however, they show limited survival after transplantation, which may be related to the internal environment.⁷ Additionally, the harsh pulmonary microenvironment inhibits the repair of damaged tissue by autologous LMSCs. Oxidative stress is one of the key underlying factors of IPF pathogenesis and is also a critical factor that leads to apoptosis.^{8,9} Thus, agents that enhance the antioxidant capacity of LMSCs are needed.

Curcuma longa L. (*curcuma aromatica*) is a yellow substance that is commonly used for food coloring, an ingredient in curry, and a Chinese medicinal herb. Curcumin (CUR) is one of the main chemical constituents of *curcuma aromatica*. A multi-effective monomer, CUR has been shown to have antioxidant, antithrombotic, and anti-inflammatory activities.¹⁰

Furthermore, CUR has been used in many preclinical studies, for which both internal sickness and external wounds have been reported.^{11–13} Several investigations have indicated that CUR decreased the release of superoxide and nitric oxide (NO), contributing to its protective effect against oxidative stress.^{14–16} However, there is some evidence that CUR acts as a growth suppressor of partially malignant cells by inducing apoptosis *via* inactivating protein kinase B (PKB/Akt), downregulating inhibitor of apoptosis proteins (IAPs), and activating the intrinsic apoptotic pathway *via* generating reactive oxygen species (ROS).¹⁷ Moreover, recent studies of IPF have demonstrated that CUR has potential antifibrotic activity, which was accompanied by increased apoptosis in primary epithelial cells and fibroblasts.¹⁸ Thus, CUR may play a dual role in oxidative stress. This study investigated the effects and possible mechanisms of action of CUR in LMSCs. Additionally, the efficacy of CUR was compared with that of the classical antioxidant N-Acetyl-L-cysteine (NAC).

Materials and methods

Animals and reagents

Healthy male C57BL/6 mice (n = 3, weight: 18 ± 2 g, age: 5-week-old) were provided by Guangdong Provincial Hospital of Traditional Chinese Medicine (Guangdong, China). CUR, NAC, 3% hydrogen peroxide (H₂O₂), dimethyl sulfoxide (DMSO), and

methylthiazolyldiphenyl-tetrazolium bromide (MTT) were purchased from Sigma-Aldrich (St. Louis, MO, USA). Alpha-Minimum Eagle's Medium (α -MEM), fetal bovine serum (FBS), penicillin-streptomycin, and 0.25% trypsin-EDTA were obtained from Gibco (Grand Island, NY, USA). Primary antibodies against B-cell lymphoma-2 (Bcl-2), Bcl-2 associated x (Bax), cleaved caspase-3, Akt, phosphorylated-Akt (p-Akt), heme oxygenase-1 (HO-1), and nuclear factor erythroid-2-related factor 2 (Nrf2) were obtained from Cell Signaling Technology (Danvers, MA, USA). The Annexin V-FITC Apoptosis Detection Kit and Mitochondrial Membrane Potential Detection Kit (5,5',6,6'-Tetrachloro-1,1',3,3'-tetraethyl-imidacarbo-cyanine, JC-1) were purchased from Beyotime Biotechnology Research Institute (Shanghai, China). This study was approved by Animal Ethics Committee of Guangdong Provincial Hospital of Traditional Chinese Medicine.

Cell extraction, culture, and identification

The mice were sacrificed by cervical dislocation and immersed in 75% ethanol for 10 minutes. Then the chest cavity was opened using sterile scissors to obtain the lungs. The trachea and bronchi were removed, and lung tissue was cut into small pieces. The chopped lung tissue was then placed in α -MEM containing 0.5 mg/mL of type II collagenase (Sigma-Aldrich) and incubated at 37°C with 5% CO₂ for 90 minutes. The incubated tissue was then gently ground and filtered through a 70- μ m cell strainer, and the filtrate was centrifuged at 377 \times g for 15 minutes. Subsequently, the supernatant was removed, and the cell pellet was cultured in α -MEM supplemented with 10% FBS and 1% penicillin/streptomycin at 37°C with 5% CO₂. The culture medium was changed every 3 days. When adherent cells reached 70%–80% confluency, they were

passed following digestion with 0.25% trypsin-EDTA. Phenotypic evaluations were performed at passage 10 by flow cytometry, and tenth- through fifteenth-generation cells were used for subsequent studies.

Cell viability assay

Murine LMSCs were plated in 96-well plates at a seeding density of 8×10^5 cells/mL and incubated for 48 hours. The cells were then exposed to 200, 400, 600, 800, and 1000 μ M H₂O₂ for 6 hours. Subsequently, 10 μ L of MTT was added to each well and incubated at 37°C for 4 hours. After replacing the liquid in the wells with 150 μ L of DMSO, the plates underwent gentle shaking for 10 minutes in the dark, after which the absorbance was measured at 490 nm. Additionally, cells were plated for 24 hours and treated with media supplemented with 2.5, 5, 10, and 20 μ M CUR or 5 mM NAC for another 24 hours. Subsequently, these cells were exposed to an appropriate dose of H₂O₂ for 6 hours, and then cell viability was measured as above.

Apoptosis assay

Cells were plated in 6-well plates at a seeding density of 8×10^5 cell/mL, incubated for 24 hours, and then divided into groups. After the corresponding treatments, the cells were collected and centrifuged at 168 \times g for 5 minutes. Next, the supernatant was discarded, and the cells were washed three times with phosphate-buffered saline (PBS). Subsequently, the cells were resuspended in 195 μ L of Annexin V-FITC binding solution, followed by adding 5 μ L of Annexin V-FITC and 10 μ L of propidium iodide. The cell suspensions were gently mixed and incubated at room temperature for 20 minutes in the dark. Finally, apoptotic cells were detected by FC500 flow cytometry (Beckman Coulter, Brea, CA, USA).

Intracellular ROS assay

Cells in each group were inoculated into 6-well plates and cultured for 24 hours. For the assay, 1 mL of 2',7'-dichlorodihydrofluorescein diacetate (DCFH-DA; diluted 1000-fold in α -MEM) was added to each well and incubated with the cells at 37°C with 5% CO₂ for 20 minutes. Extracellular DCFH-DA was removed by washing with PBS, and then the cells were collected and centrifuged at 168 ×g for 5 minutes. Finally, the cells were resuspended in 200 μ L of PBS and detected by FC500 flow cytometry.

Mitochondrial membrane potential (MMP)

After the cells from each group had adhered to 6-well plates, 1 mL of JC-1 staining solution and 1 mL of basic medium were added to the plates and incubated at 37°C with 5% CO₂ for 20 minutes. Next, the plates were centrifuged to separate the upper clear liquid, and the cells were resuspended in JC-1 staining buffer. JC-1 is an ideal fluorescent probe that is widely used to detect MMP and in this study, was measured by FC500 flow cytometry.

Western blotting

Cells were incubated in radio-immunoprecipitation assay (RIPA) buffer overnight with rocking at 4°C and were then centrifuged at 21913 ×g for 30 minutes at 4°C. The protein concentration of lysates was measured using the Protein Concentration Assay kit (LIANKE Biotech, Co. Ltd, Hangzhou, China). The lysates were then separated by SDS-PAGE and transferred to polyvinylidene fluoride (PVDF) membranes. Membranes were blocked with western blocking buffer (Beyotime Biotechnology, Shanghai, China) for 90 minutes at room temperature. After incubation with primary antibodies

overnight at 4°C, and then secondary antibodies for 1 hour at room temperature, immunoreactive bands were detected by chemiluminescence, and the grey values were analyzed with IMAGE J software.

Statistical analysis

All acquired data are expressed as mean \pm standard deviation, and data between groups were evaluated by the one-way ANOVA test using IBM SPSS Statistics for Windows, version 21.0 (IBM Corp., Armonk, NY, USA). $P < 0.05$ was considered statistically significant.

Results

Molecular characteristics of CUR and the identification of MLMSCs

The molecular weight of CUR is 368.39, and its structure is shown in Figure 1a. Additionally, first generation murine LMSCs were indistinct and mixed with a few epithelioid cells (Figure 1b). However, when these cells were passaged to the tenth generation, they presented as typical fusiform-type. Furthermore, as shown by flow cytometry analysis, Sca-1, CD54, and CD44 were expressed in the tenth generation murine LMSCs, while CD45 and CD11b were absent (Figure 1c).

CUR restored the viability of H₂O₂-treated LMSCs

Compared with the control group, the survival of murine LMSCs was gradually reduced as the H₂O₂ dose increased, becoming 51% at 600 μ M H₂O₂, which was selected as the appropriate dose for modeling (Figure 2a; * $P < 0.05$, ** $P < 0.01$). In contrast, CUR and NAC treatment significantly increased the cell viability compared with H₂O₂-treated cells ($^{##}P < 0.01$); however, all treatment groups showed decreased

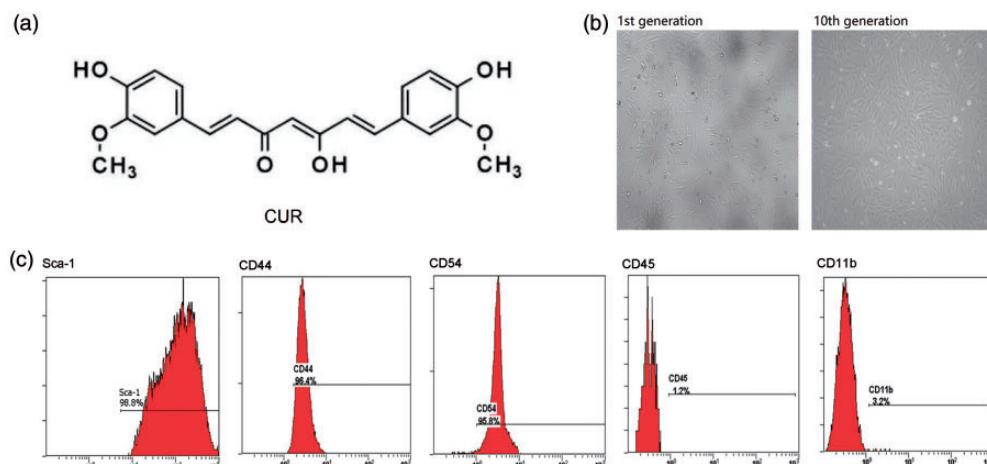


Figure 1. Characteristics of curcumin (CUR) and murine LMSCs. (a) Chemical structure of CUR. (b) Morphological characteristics of murine LMSCs (magnification: 10 \times). (c) Identification of murine LMSCs by flow cytometry.

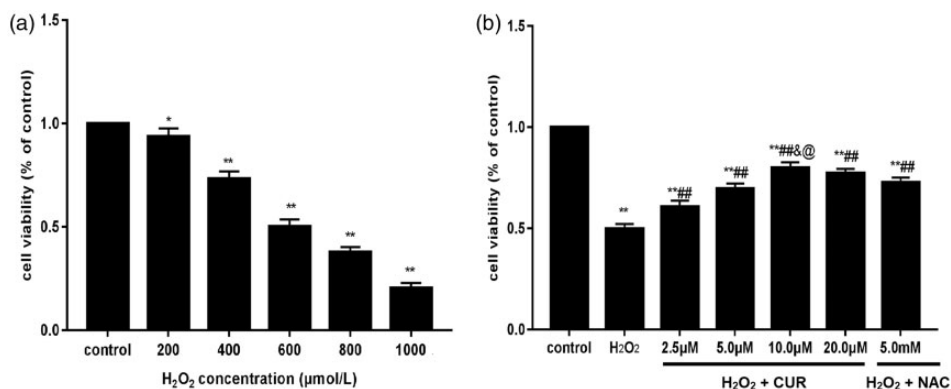


Figure 2. Effects of H_2O_2 , CUR, and NAC on the viability of murine LMSCs. (a) The cytotoxicity of various concentrations of H_2O_2 on murine LMSCs was determined by the MTT assay. (b) The protective effects of CUR and NAC on the viability of murine LMSCs. Data were obtained from three independent experiments and are expressed as mean \pm SD; * P < 0.05, ** P < 0.01 vs. control; ### P < 0.01 vs. H_2O_2 groups; & P > 0.05 vs. 20 μM CUR; @ P < 0.05 vs. NAC.

viability compared with control cells (** P < 0.01) (Figure 2b). There was no significant difference between the 10 and 20 μM CUR groups, and the NAC group showed lower viability than the 10 μM CUR group (@ P < 0.05).

CUR mitigated H_2O_2 -induced apoptosis

As shown in Figure 3, the apoptosis rate of the H_2O_2 group was $24.46\% \pm 1.35\%$, the NAC group was $12.63\% \pm 0.35\%$, and the 2.5, 5, and 10 μM CUR groups were

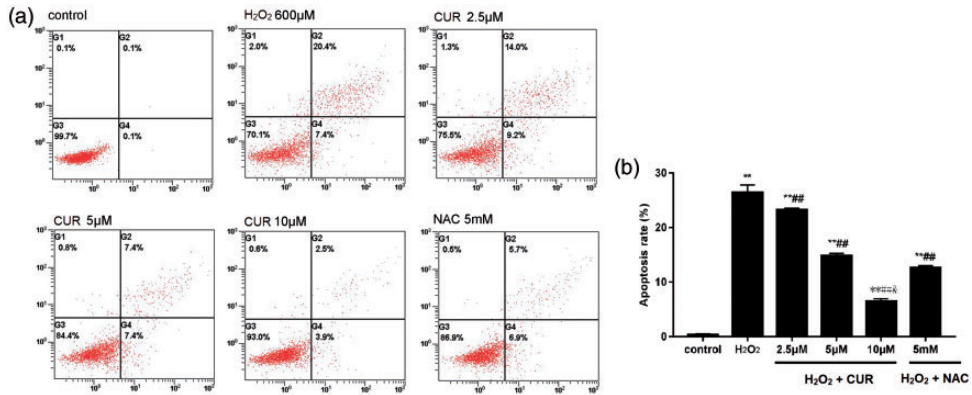


Figure 3. Effects of CUR and NAC on H₂O₂-induced apoptosis. (a) The apoptosis rates of murine LMSCs were detected by flow cytometry. (b) Quantitative analysis of the percentage of apoptotic cells. Percentage of apoptotic cells was calculated as the sum of the percentages of early- and late-stage apoptotic cells. Data were obtained from three independent experiments and are expressed as mean \pm SD; ***P* < 0.01 vs. control; ##*P* < 0.01 vs. H₂O₂; &*P* < 0.01 vs. NAC.

23.27% \pm 0.31%, 14.87% \pm 0.41%, and 6.47% \pm 0.50%, which were all higher than the control group (0.33% \pm 0.15%; ***P* < 0.01). Furthermore, the CUR and NAC groups were significantly different than the H₂O₂ group (##*P* < 0.01). CUR inhibited apoptosis in a dose-dependent manner, and 10 μ M CUR was lower than NAC (&*P* < 0.01).

CUR reduced intracellular ROS levels

Intracellular ROS levels were 16.37% \pm 1.11% in the H₂O₂ group, 8.43% \pm 0.29% in the NAC group, and 13.00% \pm 1.28%, 9.83% \pm 0.59%, and 6.23% \pm 0.35% in the 2.5, 5, and 10 μ M CUR groups, respectively, which were all significantly increased compared with the intracellular ROS levels of the control group (4.40% \pm 0.82%; ***P* < 0.01, **P* < 0.05). The CUR and NAC groups were significantly different compared with the H₂O₂ group (##*P* < 0.01), and the ROS level in the 10 μ M CUR group was significantly lower than in the NAC group (&*P* < 0.01) (Figure 4).

CUR improved mitochondrial function

As shown in Figure 5, the MMP level of the control group was 19.92% \pm 1.20%, which rapidly decreased to 1.97% \pm 0.37% in the H₂O₂ group. MMP levels were 2.57% \pm 0.25%, 3.95% \pm 0.81%, and 6.55% \pm 0.97% in the 2.5, 5, and 10 μ M CUR groups, respectively, and 3.84% \pm 0.28% in the NAC group. Compared with the control group, all treatment groups were significantly decreased (***P* < 0.01), and these results were more pronounced in the CUR and NAC groups (#*P* < 0.05, ##*P* < 0.01).

Effects of CUR on Bax, Bcl-2, and cleaved caspase-3 protein levels

As shown in Figure 6, compared with the control group, cleaved caspase-3 protein levels and the Bcl-2/Bax ratio were significantly increased in the H₂O₂, NAC, and CUR groups. The H₂O₂ and 2.5 μ M CUR groups were lower than the control group, and the 5 and 10 μ M CUR groups and the NAC group showed more pronounced

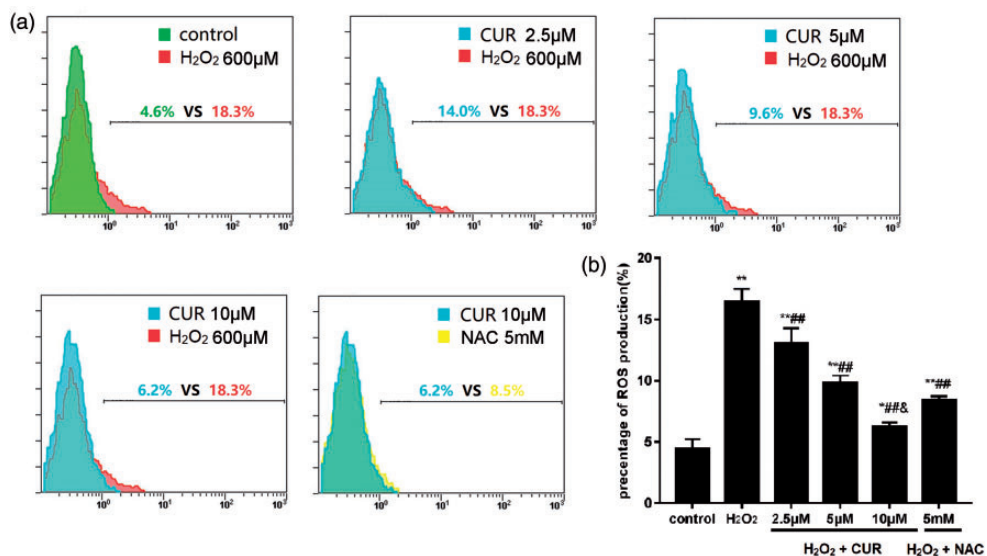


Figure 4. Effects of CUR and NAC on intracellular ROS production. (a) ROS levels in murine LMSCs were evaluated by flow cytometry. (b) Quantitative analysis of the percentage of intracellular ROS production. Percentages of ROS were calculated as intracellular oxidized matter. Data were obtained from three independent experiments and are expressed as mean \pm SD; ***P* < 0.01, **P* < 0.05 vs. control; ###*P* < 0.01 vs. H₂O₂; &*P* < 0.01 vs. NAC.

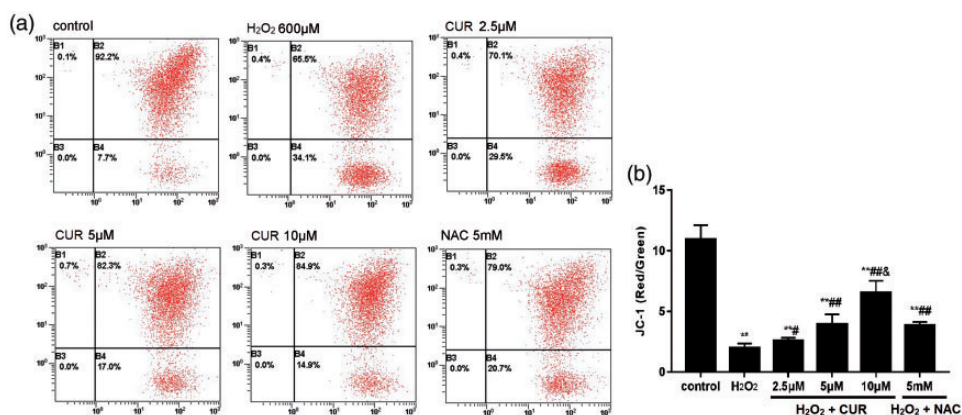


Figure 5. Effects of CUR and NAC on MMP. (a) The MMP levels of murine LMSCs were measured by flow cytometry. (b) Quantitative analysis of the percentage of MMP levels. Percentages of MMP were calculated as the ratio of JC-1 aggregates to monomers. Data were obtained from three independent experiments and are expressed as mean \pm SD; ***P* < 0.01 vs. control; #*P* < 0.05, ###*P* < 0.01 vs. H₂O₂; &*P* < 0.01 vs. NAC.

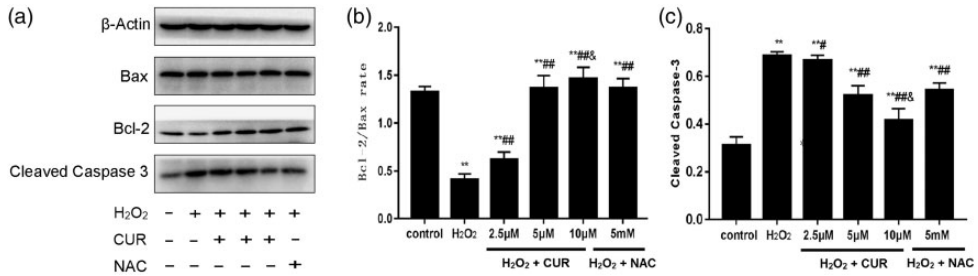


Figure 6. Effects of CUR and NAC on Bax, Bcl-2, and cleaved caspase-3 levels in murine LMSCs. (a) Protein levels of Bax, Bcl-2, and cleaved caspase-3 were assessed by western blotting. (b) Quantitative analysis of the Bax/Bcl-2 ratios. (c) Quantitative analysis of cleaved caspase-3 levels. Data were obtained from three independent experiments and are expressed as mean \pm SD; * $P < 0.01$ vs. control; # $P < 0.05$, ## $P < 0.01$ vs. H₂O₂; $\Delta P < 0.01$ vs. NAC.

differences. All CUR groups and the NAC group showed higher Bcl-2/Bax ratios and lower cleaved caspase-3 expression than the H₂O₂ group (# $P < 0.05$, ## $P < 0.01$). Compared with the NAC group, the Bcl-2/Bax ratio was significantly increased and cleaved caspase-3 expression was significantly decreased in the 10 μ M CUR group ($\Delta P < 0.01$).

Effects of CUR on the Akt/Nrf2/HO-1 signaling pathway

The p-Akt/Akt ratio and Nrf2 and HO-1 levels were significantly increased in the CUR groups and the NAC group compared with the control group (* $P < 0.05$, ** $P < 0.01$), but were significantly decreased in the H₂O₂ group (## $P < 0.01$). The p-Akt/Akt ratio and levels of Nrf2 and HO-1 were increased in a dose-dependent manner in all CUR groups. Compared with the NAC group, the 10 μ M CUR group showed higher levels of Nrf2 and HO-1 ($\Delta P < 0.01$), but the p-Akt/Akt ratio was not significantly different (Figure 7).

Discussion

IPF is a progressive fibrosing interstitial pneumonia, in which healthy lung tissue

is gradually replaced by growing scars. Furthermore, the alveolar structure is destroyed, which disrupts gas exchange to a degree that ultimately becomes life-threatening.¹⁹ Currently, epithelial cell dysfunction and abnormal epithelial-mesenchymal signaling is thought to activate fibroblasts to deposit and remodel the extracellular matrix, eventually leading to fibrotic changes.²⁰ This chronic activation is possibly related to oxidative stress, inflammatory reactions, aging, and immunity.²¹⁻²⁴ Currently, there is no effective drug for IPF, and the optimal treatment is lung transplantation. MSCs are a type of mesodermal adult stem cell that are widely distributed in connective tissues and organ stroma. MSCs show self-replicating, multi-directional differentiation, and regenerative capacities in damaged organs and tissues.⁶ They can also migrate to injured site, repair defective tissue through proliferation and directional differentiation, and secrete factors that activate other repair mechanism.²⁵ Thus, MSC therapy may replace lung transplantation as a better treatment for IPF. However, the pathological environment of IPF can affect the survival of MSCs, of which oxidative stress is a key factor.²⁶

Oxidative stress refers to an imbalance between oxidation and anti-oxidation *in vivo* that causes oxidation and produces

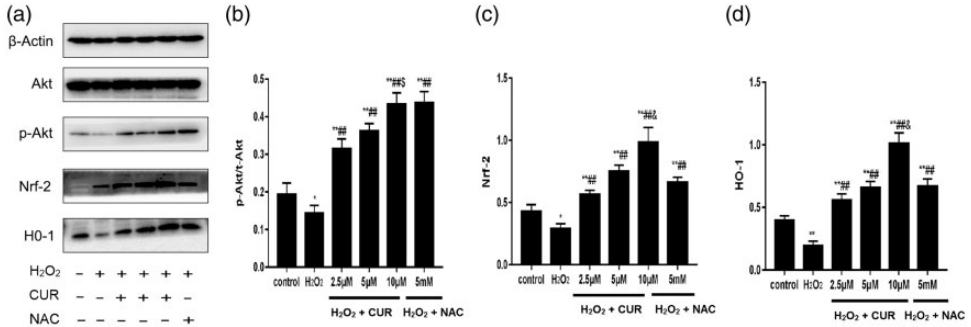


Figure 7. Effects of CUR and NAC on the Akt/Nrf2/HO-1 pathway in murine LMSCs. (a) Protein levels of Akt, p-Akt, Nrf2, and HO-1 were assessed by western blotting. (b) Quantitative analysis of p-Akt/Akt ratios. (c) Quantitative analysis of Nrf2 levels. (d) Quantitative analysis of HO-1 levels. Data were obtained from three independent experiments and are expressed as mean \pm SD; * P < 0.05, ** P < 0.01 vs. control; ### P < 0.01 vs. H₂O₂; \$ P > 0.05, & P < 0.01 vs. NAC.

a large number of oxidative intermediates, including ROS, which can negatively impact signal transduction and the maintenance of physiological function. As H₂O₂ is a strong oxidant, we chose it in this study to simulate the oxidative stress of the IPF microenvironment. The viability of murine LMSCs was significantly reduced after H₂O₂ exposure, decreasing to 51% with 600 μM H₂O₂, which was selected as the modeling density. Additionally, excessive ROS resulted in apoptosis, which was closely related to mitochondrial dysfunction.²⁷ This study found that CUR could restore the viability of murine LMSCs and reduce their level of oxidative stress-induced apoptosis to a better degree than NAC. Furthermore, CUR pretreatment reduced intracellular ROS production and improved the MMP of murine LMSCs. MMP is required for oxidative phosphorylation and ATP production; thus, MMP indirectly reflects mitochondrial status. Taken together, CUR was shown to enhance the antioxidant capacity of murine LMSCs, and was superior to the classical and powerful antioxidant NAC.

Bax and Bcl-2 belong to the Bcl-2 gene family, which plays key roles in regulating apoptosis. Bax and Bcl-2 regulate the

stability of the mitochondrial structure, and function through synergistic action with other apoptotic proteins. The Bcl-2 family includes two types of proteins: anti-apoptotic proteins, such as Bcl-2, and pro-apoptotic proteins, such as Bax. In the early stage of apoptosis, the pro-apoptotic proteins form pores in the outer mitochondrial membrane by homologous oligomerization, resulting in cytochrome-c release and eventually caspase activation and apoptosis.^{28,29} This study found that levels of the anti-apoptotic protein Bcl-2 were decreased, while levels of the pro-apoptotic proteins Bax and cleaved caspase-3 were increased under oxidative stress. These results suggested that oxidative stress weakened the inhibition of apoptosis in LMSCs, while proteins that promoted apoptosis were enhanced. With CUR pretreatment, the Bcl-2/Bax ratio was increased, and caspase-3 expression was decreased, which further confirmed the protective effect of CUR on the viability of LMSCs.

Nrf2 belongs to the alkaline leucine zipper family and is a widely expressed transcription factor *in vivo* that has strong antioxidant capacity, primarily through HO-1 activation. Akt plays an important role in cell survival and apoptosis and participates

in the activation and nuclear translocation of Nrf2 through phosphorylation.³⁰ The Akt/Nrf2/HO-1 pathway is closely related to oxidative stress and apoptosis. Several studies have described agents that alleviate cellular oxidative damage through this pathway.^{31–33} In this study, CUR was found to promote Akt phosphorylation, increase the p-Akt/Akt ratio, and increase Nrf2 expression, leading to increased HO-1 release. Thus, this pathway may underlie the antioxidant effect of CUR.

Conclusion

In summary, CUR was demonstrated to have an antioxidant protective effect on murine LMSCs that may be related to the Akt/Nrf2/HO-1 signaling pathway. Additionally, H₂O₂-mediated mitochondrial damage was observed, which could potentially affect mitochondrial fusion, function, and/or autophagy; these potential effects will be the focus of future studies.


Declaration of conflicting interest

The authors declare that there is no conflict of interest.

Funding

This work was supported by grants from the National Natural Science Foundation of China (No. 81560765, No. 81660760, and No. 81860826), the Technology Research and Development Program of the Education Department of Jiangxi Province (No. GJJ150851), the Technology Research and Development Program of the Science and Technology Department of Jiangxi Province (No. 20171BAB215056), and the Postgraduate Innovation Project of Jiangxi Province (YC2018-B075).

ORCID iD

Liangji Liu  <https://orcid.org/0000-0001-9567-0063>

References

1. Xaubet A, Ancochea J and Molina-Molina M. Idiopathic pulmonary fibrosis. *Med Clin (Barc)* 2017; 148: 170–175.
2. Martinez FJ, Collard HR, Pardo A, et al. Idiopathic pulmonary fibrosis. *Nat Rev Dis Primers* 2017; 20: 17074.
3. Akram KM, Samad S, Spiteri MA, et al. Mesenchymal stem cells promote alveolar epithelial cell wound repair in vitro through distinct migratory and paracrine mechanisms. *Respir Res* 2013; 14: 9.
4. Cappetta D, De Angelis A, Spaziano G, et al. Lung mesenchymal stem cells ameliorate elastase-induced damage in an animal model of emphysema. *Stem Cells Int* 2018; 2018: 9492038.
5. Lan YW, Choo KB, Chen CM, et al. Hypoxia-preconditioned mesenchymal stem cells attenuate bleomycin-induced pulmonary fibrosis. *Stem Cell Res Ther* 2015; 6: 97.
6. Harpole M, Davis J and Espina V. Current state of the art for enhancing urine biomarker discovery. *Expert Rev Proteomics* 2016; 13: 609–626.
7. Lou G, Song X, Yang F, et al. Exosomes derived from miR-122-modified adipose tissue-derived MSCs increase chemosensitivity of hepatocellular carcinoma. *J Hematol Oncol* 2015; 8: 122.
8. Brandl A, Meyer M, Bechmann V, et al. Oxidative stress induces senescence in human mesenchymal stem cells. *Exp Cell Res* 2011; 317: 1541–1547.
9. Cheresh P, Kim SJ, Tulasiram S, et al. Oxidative stress and pulmonary fibrosis. *Biochim Biophys Acta* 2013; 1832: 1028–1040.
10. Perkins K, Sahy W and Beckett RD. Efficacy of curcuma for treatment of osteoarthritis. *J Evid Based Complementary Altern Med* 2017; 22: 156–165.
11. Lelli D, Sahebkar A, Johnston TP, et al. Curcumin use in pulmonary diseases: state of the art and future perspectives. *Pharmacol Res* 2017; 115: 133–148.
12. Kunnumakkara AB, Bordoloi D, Harsha C, et al. Curcumin mediates anticancer effects by modulating multiple cell signaling pathways. *Clin Sci (Lond)* 2017; 131: 1781–1799.

13. Mohanty C and Sahoo SK. Curcumin and its topical formulations for wound healing applications. *Drug Discov Today* 2017; 22: 1582–1592.
14. Samarghandian S, Azimi-Nezhad M, Farkhondeh T, et al. Anti-oxidative effects of curcumin on immobilization-induced oxidative stress in rat brain, liver and kidney. *Biomed Pharmacother* 2017; 87: 223–229.
15. Wang N, Wang F, Gao Y, et al. Curcumin protects human adipose-derived mesenchymal stem cells against oxidative stress-induced inhibition of osteogenesis. *J Pharmacol Sci* 2016; 132: 192–200.
16. Rashid K, Chowdhury S, Ghosh S, et al. Curcumin attenuates oxidative stress induced NF κ B mediated inflammation and endoplasmic reticulum dependent apoptosis of splenocytes in diabetes. *Biochem Pharmacol* 2017; 143: 140–155.
17. Kuttikrishnan S, Siveen KS, Prabhu KS, et al. Curcumin induces apoptotic cell death via inhibition of PI3-Kinase/AKT pathway in B-Precursor acute lymphoblastic leukemia. *Front Oncol* 2019; 9: 484.
18. Rodriguez LR, Bui SN, Beuschel RT, et al. Curcumin induced oxidative stress attenuation by N-acetylcysteine co-treatment: a fibroblast and epithelial cell in-vitro study in idiopathic pulmonary fibrosis. *Mol Med* 2019; 25: 27.
19. Richeldi L, Collard HR and Jones MG. Idiopathic pulmonary fibrosis. *Lancet* 2017; 389: 1941–1952.
20. Wolters PJ, Collard HR and Jones KD. Pathogenesis of idiopathic pulmonary fibrosis. *Annu Rev Pathol* 2014; 9: 157–179.
21. Hosseinzadeh A, Javad-Moosavi SA, Reiter RJ, et al. Oxidative/nitrosative stress, autophagy and apoptosis as therapeutic targets of melatonin in idiopathic pulmonary fibrosis. *Expert Opin Ther Targets* 2018; 22: 1049–1061.
22. Liu G, Cooley MA, Jarnicki AG, et al. Fibulin-1c regulates transforming growth factor- β activation in pulmonary tissue fibrosis. *JCI Insight* 2019; 5: 124529.
23. Pardo A and Selman M. Lung fibroblasts, aging, and idiopathic pulmonary fibrosis. *Ann Am Thorac Soc* 2019; 13: S417–S421.
24. Chanda D, Otoupalova E, Smith SR, et al. Developmental pathways in the pathogenesis of lung fibrosis. *Mol Aspects Med* 2019; 65: 56–69.
25. Birbrair A. Stem cell microenvironments and beyond. *Adv Exp Med Biol* 2017; 1041: 1–3.
26. Fois AG, Paliogiannis P, Sotgia S, et al. Evaluation of oxidative stress biomarkers in idiopathic pulmonary fibrosis and therapeutic applications: a systematic review. *Respir Res* 2018; 19: 51.
27. Veith C, Boots AW, Idris M, et al. Redox imbalance in idiopathic pulmonary fibrosis: a role for oxidant cross-talk between NADPH oxidase enzymes and mitochondria. *Antioxid Redox Signal* 2019; 31: 1092–1115.
28. Nkpaa KW, Awogbindin IO, Amadi BA, et al. Ethanol exacerbates manganese-induced neurobehavioral deficits, striatal oxidative stress, and apoptosis via regulation of p53, caspase-3, and Bax/Bcl-2 ratio-dependent pathway. *Biol Trace Elem Res* 2019; 191: 135–148.
29. Suzuki K, Yanagihara T, Yokoyama T, et al. Bax-inhibiting peptide attenuates bleomycin-induced lung injury in mice. *Biol Open* 2017; 6: 1869–1875.
30. Tai W, Deng S, Wu W, et al. Rapamycin attenuates the paraquat-induced pulmonary fibrosis through activating Nrf2 pathway. *J Cell Physiol* 2019; 235: 1759–1768.
31. Li W, Cai ZN, Mehmood S, et al. Polysaccharide FMP-1 from *Morchella esculenta* attenuates cellular oxidative damage in human alveolar epithelial A549 cells through PI3K/AKT/Nrf2/HO-1 pathway. *Int J Biol Macromol* 2018; 120: 865–875.
32. Cui W, Leng B and Wang G. Klotho protein inhibits H₂O₂-induced oxidative injury in endothelial cells via regulation of PI3K/AKT/Nrf2/HO-1 pathways. *Can J Physiol Pharmacol* 2019; 97: 370–376.
33. Dai H, Wang P, Mao H, et al. Dynorphin activation of kappa opioid receptor protects against epilepsy and seizure-induced brain injury via PI3K/Akt/Nrf2/HO-1 pathway. *Cell Cycle* 2019; 18: 226–237.